Differences And Similarities In The Cocos-North America and Cocos-Caribbean Convergence, as Revealed by Seismic...

Article *in* Journal of South American Earth Sciences · October 2015

DOI: 10.1016/j.jsames.2015.10.002

2 authors, including:

F. Ramón Zúñiga
Universidad Nacional Autónoma de México
99 PUBLICATIONS **929** CITATIONS

Journal of South American Earth Sciences xxx (2015) 1–13

Contents lists available at ScienceDirect

Journal of South American Earth Sciences

journal homepage: www.elsevier.com/locate/jsames

Differences and similarities in the Cocos–North America and Cocos–Caribbean convergence, as revealed by seismic moment tensors

Marco Guzmán-Speziale*, F. Ramón Zúñiga

Centro de Geociencias, Universidad Nacional Autónoma de México, Blvd. Juriquilla 3001, Querétaro 76230, Mexico

ARTICLE INFO

Article history:
Received 22 January 2015
Received in revised form
21 September 2015
Accepted 2 October 2015
Available online xxx

Keywords:
Seismicity
Plate convergence
Centroid moment-tensor solutions
North America plate
Cocos-plate
Caribbean plate

ABSTRACT

We investigate the differences and similarities in Cocos–North America and Cocos–Caribbean convergence, reflected by seismicity and seismic moment. We use well-located hypocenters of earthquakes in the convergence margin, as well as within the subducted slab. We sort these data by number of events in the two converging margins, and by their magnitudes. We also use this database to determine an improved geometric model of the subducted slab. We find a shallow-dipping subducting Cocos plate underneath North America and a steeper dip slab under the Caribbean plate. The transition between them appears to be smooth.

Centroid Moment tensor solutions indicate that almost all of the thrust-faulting earthquakes along Cocos–North America take place at shallow depths. Normal-faulting events along this margin only take place to depths of 100 km. Thrust- and normal-faulting events take place at all depths along the Cocos–Caribbean margin. Cummulative scalar seismic moment for shallow, thrust-faulting events, is larger along Cocos–North America.

T axes of intermediate-depth, normal- and thrust-faulting events show that the subducted Cocos plate is in maximum tension along the direction of maximum dip. Azimuth of earthquake slip vectors for shallow events along the Cocos–North America margin agree well with the direction of plate convergence. They do not agree along the Cocos–Caribbean margin; instead, agreement is found with Cocos–North America relative plate motion.

Compensated Linear Vector Dipole (CLVD) ratio, which measures how different a seismic source is from a pure double-couple, along both margins is inversely proportional to scalar seismic moment, indicating that for larger magnitudes rupture is closer to a double-couple mechanism than at smaller moments.

1. Introduction

The Middle America trench (MAT) serves as a plate boundary between the subducting Cocos (Coco) and overriding North America (Noam) and Caribbean (Carb) plates, (Fig. 1). The plate boundary between Noam and Carb is defined by the Swan and Motagua-Polochic (Motagua for short) fault zones (Fig. 1), although it is not clear where or how (or if at all), the Motagua-Polochic reaches the MAT. Consequently, the transition in overriding plate for the subduction of the Cocos plate is not clearly defined, but many authors agree that it is located somewhere around longitude −96° (Fig. 1) (e.g., Malfait and Dinkelman, 1972; Muehlberger and Ritchie, 1975; Plafker, 1976; Burkart, 1978, 1983). Guzmán-Speziale et al. (1989) and Guzmán-Speziale and Meneses-Rocha (2000) define the triple junction of the three plates as a wide zone of deformation which spans most of the state of Chiapas, in Mexico (Fig. 1); this would extend the overriding Caribbean plate to the west, to about longitude −96°.

There have been several GPS studies in the area in recent years (e.g., DeMets et al., 2000; DeMets, 2001; Lyon-Caen et al., 2006; DeMets et al., 2007; LaFemina et al., 2009; Rodriguez et al., 2009; Franco et al., 2012). Only two of them directly address the plate boundary problem. Lyon-Caen et al. (2006) propose that the triple junction covers a wedge-shaped area 400 km wide south of the Motagua-Polochic system and includes a coastal microplate between the Middle America trench and the Central American

* Corresponding author.
E-mail addresses: marco@geociencias.unam.mx (M. Guzmán-Speziale), ramon@geociencias.unam.mx (F.R. Zúñiga).

http://dx.doi.org/10.1016/j.jsames.2015.10.002
0895-9811/

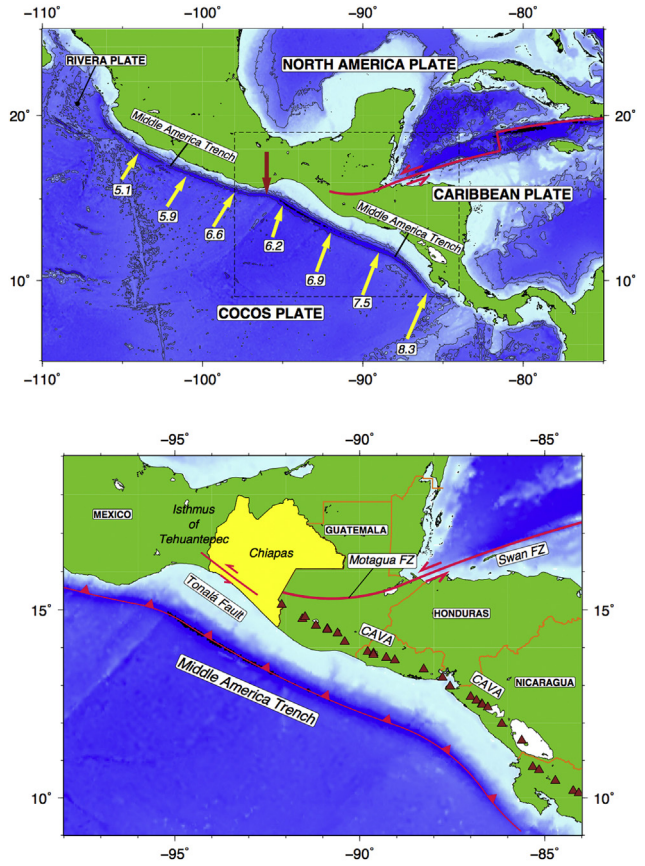

Fig. 1. Tectonic framework of the Cocos plate convergent margin. Top- General view. Yellow arrows indicate direction and speed (in cm/yr) of plate convergence, calculated from the Euler poles given by DeMets et al. (2010) for Coco–Noam (first three arrows, from left to right), and Coco–Carb (last four arrows). Length of arrow is proportional to speed. Red arrow shows location of the −96° longitude. Box indicates location of lower panel. Bottom- Location of features and places mentioned in text. Triangles indicate volcanoes of the Central American Volcanic Arc (*CAVA*) with known Holocene eruption (Siebert and Simkin, 2002). Figures drawn with *The Generic Mapping Tools* (Wesseel and Smith, 1991; Wessel et al., 2013). (For interpretation of the references to color in this figure legend, the reader is referred to the web version of this article.)

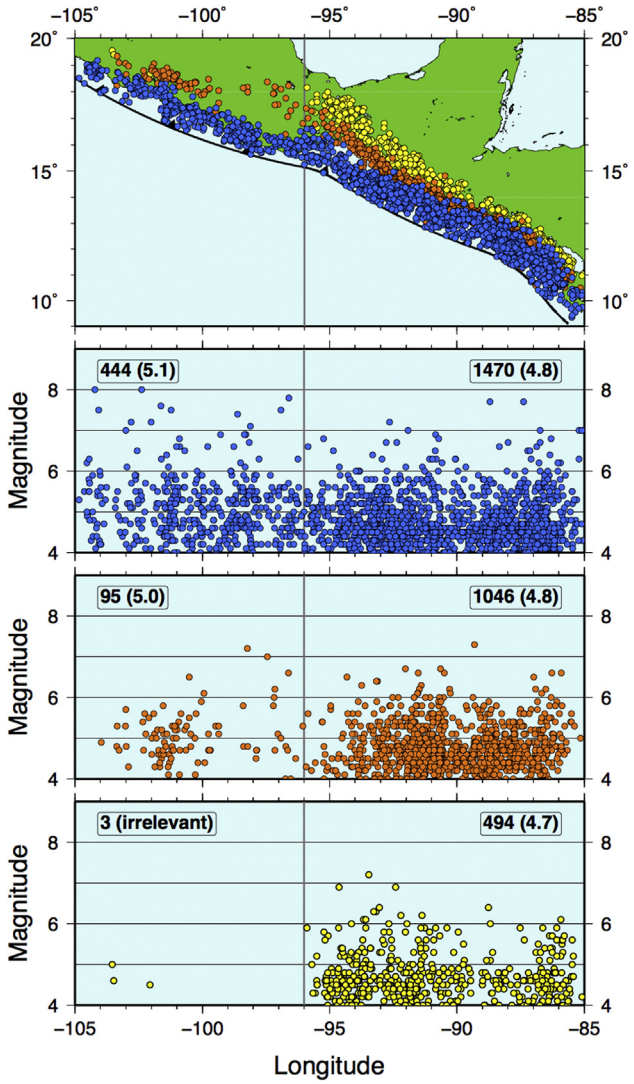

Fig. 2. Seismicity along the convergent margin. Top: Map view. Blue circles are shallow ($z \leq 60$ km) hypocenters; orange, intermediate-depth ($60 < z \leq 100$ km); yellow, deep ($z > 100$ km). Next three panels: Earthquakes as a function of longitude and magnitude for shallow (blue dots), intermediate (orange), and deep (yellow) hypocenters. Numbers indicate number of events on each convergent margin, with average magnitude in parenthesis. Gray line in this and subsequent figures mark the −96° longitude. (For interpretation of the references to color in this figure legend, the reader is referred to the web version of this article.)

volcanic arc. Franco et al. (2012) suggest that the Motagua fault may be extrapolated to the west, reaching the MAT, as the "Motagua fault west", although they do not provide evidence that this is the case.

Several authors (e.g., Bevis and Isacks, 1984; Burbach et al., 1984; Pardo and Suárez, 1995; García-Quintero, 2007) found a change in the dip of the subducting slab at longitude −96°. The shape of the trench changes abruptly here, as well: To the northwest, its maximum depth is about 4500 m and it is narrow with almost no continental platform. In contrast, from this point to the southeast the trench widens, reaches depths of about 5500 m and possesses a well-defined continental platform, 100 km in width (Fig. 1). For the purpose of this work, then, the Cocos plate is being subducted underneath the North America plate along the Middle America trench, from the Cocos–Rivera–North America triple junction (at about longitude −105°) to the Cocos–Caribbean–North America triple junction (longitude −96°). From there to about longitude −85° (where the trench looses its trace) the Cocos plate is being subducted underneath the Caribbean plate (Fig. 1).

Uyeda and Kanamori (1979) and Uyeda (1982) have argued that along plate margins of the *Chilean type*, those where the overriding plate advances towards the subducting plate, the *Wadati-Benioff zone* (that is, the subducted slab, as defined by hypocenters) is shallow-dipping, great ($M \geq 8$), shallow, thrust-faulting earthquakes occur along the plate interface, the trench is shallow, and there is a well-developed accretionary prism. In the *Mariana type*, the overriding plate is stationary with respect to the subducting plate or retreats from it, the dip of the Wadti-Benioff zone is steep, no great earthquakes take place along the interface, the trench is deep, and there is no accretionary prism. For Uyeda (1982), both modes are present along the Middle America trench: *Chilean type* along the Cocos–North America plate boundary, and *Mariana type* along the Cocos–Caribbean interface. For Jarrard (1986), however, the *Chilean* and *Mariana* types are only end member cases, with most other convergent margins on Earth occupying a continuum between these two. Based on the strain regimes of the upper-plate, Jarrard (1986) defines seven different strain classes, with number one being *active back-arc spreading* and seven *very strongly compressional*. He places Southeast Mexico in number six, *moderately compressional*, and Central America in number three, *mildly tensional*.

Please cite this article in press as: Guzmán-Speziale, M., Zúñiga, F.R., Differences and similarities in the Cocos–North America and Cocos–Caribbean convergence, as revealed by seismic moment tensors, Journal of South American Earth Sciences (2015), http://dx.doi.org/10.1016/j.jsames.2015.10.002

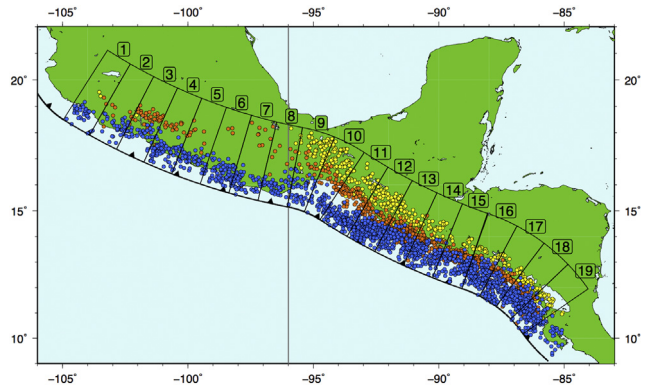

Fig. 3. Location of hypocentral cross-sections. Hypocentral depths are keyed as in previous figures.

Convergence of the Cocos plate offers a unique opportunity to study the two modes of subduction (or different *strain classes*, in the words of Jarrard, 1986) along the same trench. The difference in *mode* of subduction must be reflected in the style of faulting of earthquakes along the plate interface, as well as within the subducted slab. In this work, we use very well located hypocenters reported in the catalogs of Engdahl et al. (1998) and the International Seismological Centre (2012), and Centroid-moment tensor solutions reported by the *Global CMT Project* (e.g., Dziewonski et al., 1981; Dziewonski and Woodhouse, 1983) to determine several seismic parameters that may shed some light into the differences due to the two modes of subduction and into the transition from one mode to the other. We also take advantage of the better accuracy in hypocentral parameters of the catalogs mentioned above to determine an improved an detailed geometric model of the subducted Cocos plate.

2. Tectonic framework

Convergence velocity between the Cocos and North America plates (e.g., DeMets et al., 2010) goes from about 5 cm/yr to 7 cm/yr, whereas the Cocos and Caribbean plates move from 6 cm/yr to more than 8 cm/yr (Fig. 1). In an absolute or no-net-rotation reference frame, the North America plate moves towards the subducting Cocos plate, whereas the Caribbean plate is essentially stationary or very slowly moving away from the Cocos plate (e.g., Minster and Jordan, 1978; DeMets et al., 1990; Gripp and Gordon, 1990, 2002; DeMets, 2001; Bird, 2003; Argus et al., 2011; Becker et al., 2015).

Both plate margins are seismically active (e.g., Burbach et al., 1984; LeFevre and McNally, 1985; Singh and Mortera, 1991; Kostoglodov and Ponce, 1994; Pardo and Suárez, 1995; Lemoine et al., 2002; García-Quintero, 2007). Large interplate events have taken place along both interfaces (e.g, Singh and Mortera, 1991; Kostoglodov and Ponce, 1994), such as the 1932 ($M = 8.2$), or the 1985 ($M = 8.1$) events.

Several studies have tackled different aspects of the seismicity along the Middle America trench: Chael and Stewart (1982) found similarities in several parameters of a few large, interplate events along the Middle America trench; Burbach et al. (1984) analyzed seismicity and tectonics of the subducted Cocos plate; LeFevre and McNally (1985) studied the stress distribution and the effect of subduction of a seismic ridges on seismicity; Singh and Mortera (1991) determined source parameters and source-time functions of historical and recent interplate events along the Coco–Noam interface; Kostoglodov and Ponce (1994) investigated the coupling strength of the subducting Cocos plate and seismicity along what they called *the mexican part* of the Middle America trench. Pardo and Suárez (1995) determined the shape of the subducted Cocos plate and its seismic and tectonic characteristics. Rebollar et al. (1999) studied the geometry and state of stress of the subducted Cocos plate in southern Mexico. Lemoine et al. (2002) studied slab-pull and slab-push earthquakes. More recently, studies have focused on such aspects as slow-slip events (e.g., Iglesias et al., 2004; Kostoglodov et al., 2010), non-volcanic tremor (e.g., Payero et al., 2008; Husker et al., 2012; Cruz-Atienza et al., 2015), among others.

Ever since the pioneering work of Molnar and Sykes (1969), the geometry of the subducted Cocos plate has been the subject of several studies. Workers such as Hanus and Vanek (1978), Bevis and Isacks (1984), Burbach et al. (1984), LeFevre and McNally (1985), Suárez et al. (1990), Pardo and Suárez (1995), Valdés-González and Meyer (1996), Gorbatov and Fukao (2005), Pérez-Campos et al. (2008) used earthquakes (hypocentral locations, focal mechanisms, or tomography) to determine the geometry of the subducted Cocos plate, whereas Melgar and Pérez-Campos (2011) used receiver functions. Dougherty et al. (2012) modeled the structure of the subducted slab in central Mexico using waveform information and Chen and Clayton (2012) obtained a seismic model through the use of velocity and attenuation tomography. Hayes et al. (2012) obtained a three-dimensional model of several subduction zone geometries, including the subducted Cocos plate. Other authors, such as Molina-Garza and Urrutia-Fucugauchi (1993), Arzate et al. (1993, 1995), Geolimex Working Group (1994), Mena et al. (1995), Campos-Enríquez and Sánchez-Zamora (2000), Jording et al. (2000) derived the geometry from potential methods.

All of these works coincide: the subducted Cocos plate has a variable angle of subduction underneath North America that goes from 45° at the northwest to almost flat in the southeast, and a fairly uniform angle of subduction (40° to 45°) underneath the Caribbean.

3. Seismicity

Engdahl et al. (1998) relocated more than 100,000 earthquakes worldwide. The location is significantly improved from other global locations (like, for example, those of the *United States Geological Survey*) because additional phases beyond the usual *P* and *S* are used, such as the core phases *PkiKP* and *PKPdf*. The most critical parameter, depth, is the one that improves most because depth phases *pP*, *pwP*, and *sP* are used in the location procedure. Horizontal and vertical errors in this database are in the order of 5 km and 10 km, respectively. Presently, the catalog spans from 1964 to 2008. The International Seismological Centre (2012) also systematically relocates hypocenters, reported from seismic stations around the Earth; hypocenters relocated by the *ISC* are reported in their *Reviewed ISC bulletin*.

Data from the hypocentral catalog of Engdahl et al. (1998) (hereafter the *EHB* catalog), and the Reviewed ISC bulletin (International Seismological Centre, 2012) (hereafter the *ISC* catalog) are used here. Hypocenters reported in the EHB catalog span from 1964 to 2008. These data are complemented with hypocenters from the ISC catalog, in the time period 2009 to February 2012. Our combined *EHB-ISC* catalog includes then, hypocenters from 1964 to February 2012. We only use events with magnitudes 4.0 or greater.

According to Pacheco et al. (1993), the area of contact between the overriding and subducting plates (i.e., the interplate zone) extends to a depth of 40 km in the case of the Cocos–North America margin, and to 47 km for Cocos–North America. However, results presented here (see below) suggest that the depth of transition is

Please cite this article in press as: Guzmán-Speziale, M., Zúñiga, F.R., Differences and similarities in the Cocos–North America and Cocos–Caribbean convergence, as revealed by seismic moment tensors, Journal of South American Earth Sciences (2015), http://dx.doi.org/10.1016/j.jsames.2015.10.002

about 60 km.

We divide our seismic data into three depth brackets: 60 km or less, between 60 and 100 km, and deeper than 100 km. Earthquakes in the first category reflect interplate activity between subducting and overriding plates, as determined by the depth of transition; the 100 km deep is chosen mainly because it is the maximum depth of seismicity in central Mexico, and 100 or more km deep corresponds to earthquakes within the subducted slab in Central America. We further divide the data into west and east, the former related to Cocos–North America convergence, and the latter to Cocos–Caribbean. The dividing line is the −96° meridian.

Because we are not interested in crustal seismic activity within the overriding plates, shallow events ($z \leq 60$ km) we consider are only those within an angular distance of 1.5° from the Middle America trench. In order to avoid seismic activity related to Rivera-North America convergence, we only consider events east of longitude −105°.

We also use the combined *EHB-ISC* catalog to determine a new geometric model of the subducted Cocos plate. We do so by obtaining 19 contiguous seismic cross-sections perpendicular to the trench. Sections curve along the arcuate trench and hypocenters are projected onto a plane perpendicular to the curvature of the trench, within the section itself (see Guzmán-Speziale, 1995). In doing so, overlapping of contiguous sections is prevented and each hypocenter is only projected once. Details of the method may be found in Guzmán-Speziale (1995).

We fit a surface to the hypocentral data. We do so by using the routine *surface* contained in *The Generic Mapping Tools* (*GMT*) of Wessel and Smith (1991). The algorithm reads randomly distributed (*x,y,z*) values and produces gridded values of *z(x,y)* by solving (Smith and Wessel, 1990):

$$(1-T)\cdot\nabla^2\left(\nabla^2 z\right)+T\left(\nabla^2 z\right)=0 \tag{1}$$

where T is a tension factor between 0 and 1. Before fitting the surface, hypocentral vectors are block-averaged by L2 norm, using the routine *blockmean* of *GMT*.

4. Centroid-moment tensors

Worldwide Centroid-Moment Tensor solutions (CMTs) for earthquakes with magnitude greater or equal than 5.0, are routinely calculated by the *Global CMT Project* (formerly the *Harvard Centroid-Moment-Tensor Project*) since 1978 (e.g., Dziewonski et al., 1981; Ekström et al., 2012). *CMT's* provide information on the seismic moment tensor of earthquakes and hence data on such parameters as: size of earthquake (scalar seismic moment), type of faulting, magnitude and direction of principal (**T**, **B**, and **P**) axes, and *Compensated Linear Vector Dipole* (*CLVD*) which measures how different a seismic source is from a pure double-couple (e.g., Frohlich and Apperson, 1992; Julian et al., 1998; Miller et al., 1998).

We use CMTs from this database, in the time period 1978 to April 2014. In most cases, hypocentral data (latitude, longitude, depth) in the *CMT* catalog are those calculated by the *Preliminary Determination of Epicenters* (PDE) of the *United States Geological Survey*. Location errors in the PDE catalog are usually larger than in the EHB catalog. For this reason, we substitute location parameters for CMTs from our *EHB-ISC* catalog, unless this information is not available, in which case hypocentral data directly from the CMT catalog are used. As with the *EHB-ISC* catalog, shallow ($z \leq 60$ km) *CMT's* are considered if they are located on the continental side of the trench and within 1.5° of it. Again, events west of longitude −96° are considered to belong to Cocos–North America convergence, whereas those east of this longitude are taken to belong to Cocos–Caribbean.

T, **B**, and **P** axes are the three eigenvectors of the Centroid Moment tensor. Azimuth (or trend) of **T** axis indicates the horizontal direction of least compression (e.g., Jost and Herrmann, 1989). Here we obtain azimuth of **T** axes of normal-faulting, intermediate-depth ($z > 60$ km) and deep ($z > 100$ km) thrust-faulting events, to determine the direction of slab-pull within the subducted slab. At intermediate depths, slab pull is dominated by normal-faulting events, whereas at depths greater than 100 km, and given the dip of the subducted slab (cf. Sections 9–19, Fig. 4), the **T** axis plunges more steeply, yielding to thrust-faulting mechanisms.

For our analysis, *CMT* solutions are divided into type of faulting, inspired in the criteria of Frohlich and Apperson (1992): A thrust-faulting mechanism has a **T** axis plunging 45° or more, whereas the **P** axis plunges at least 45° in the case of a normal mechanism. Strike-slip mechanisms (those whose **B** axis plunges more than 45°) are not included in this study because it has been shown elsewhere that they mainly occur associated to crustal deformation in Central America (e.g., White and Harlow, 1993; Cáceres et al., 2005; Guzmán-Speziale et al., 2005). We also exclude the few *oblique* earthquakes, those whose **T**, **B**, and **P** axes all plunge less than 45°.

There are several parameters from the *CMTs* we examine to establish differences between Coco–Noam and Coco–Carb convergence:

- Number of events by type of fault, and by depth.
- Sum of scalar seismic moment.
- Trend of **P** axes for shallow, thrust-faulting events.
- Trend of **T** axes for intermediate-depth and deep normal-faulting events, as well as for deep thrust-faulting events.
- Dip of **T** axes for intermediate-depth and deep normal-faulting events, and for deep thrust-faulting events.
- *CLVD* ratio (Frohlich and Apperson, 1992)
- Horizontal component of slip vector for thrust-faulting, shallow events.

Here, number of events refers to *CMTs*, as they are classified in thrust or normal faulting events by the criteria given above. Scalar seismic moment is obtained directly from the *CMT* data, as are trends of **T** and **P** axes.

The direction of the most compressive stress is given by the azimuth of **P** axes, which we obtain for shallow, thrust-faulting earthquakes, to determine differences in compression direction bewteen the Cocos–North America and the Cocos–Caribbean margins. Plunge (dip) of **T** axes for intermediate-depth normal ervents ($z > 60$ km) and deep ($z > 100$ km) thrust-faulting events is a good indicator of the relationship between the dip of subduction and tension (or, more properly, least compression) within the subducted slab. Here we obtain plunge of **T** axes for such events to find the correlation with dip of subducted slab.

The compensated linear vector dipole ratio (*CLVD* ratio or simply f_{clvd}) (Frohlich and Apperson, 1992) is a measure of how a source differs from a pure double couple. Its value ranges from 0.0 (pure double couple) to 0.5 (pure CLVD source). It is calculated by (Frohlich and Apperson, 1992):

$$f_{clvd}=\frac{|\mathbf{m_B}|}{\max[|\mathbf{m_T}|,|\mathbf{m_P}|]} \tag{2}$$

where $\mathbf{m_T}$, $\mathbf{m_B}$, and $\mathbf{m_P}$ are the largest, intermediate, and smallest principal moments, respectively. These values are directly obtainable from the *CMT* database.

The slip vector **U** is the vector on the fault plane along which

Please cite this article in press as: Guzmán-Speziale, M., Zúñiga, F.R., Differences and similarities in the Cocos–North America and Cocos–Caribbean convergence, as revealed by seismic moment tensors, Journal of South American Earth Sciences (2015), http://dx.doi.org/10.1016/j.jsames.2015.10.002

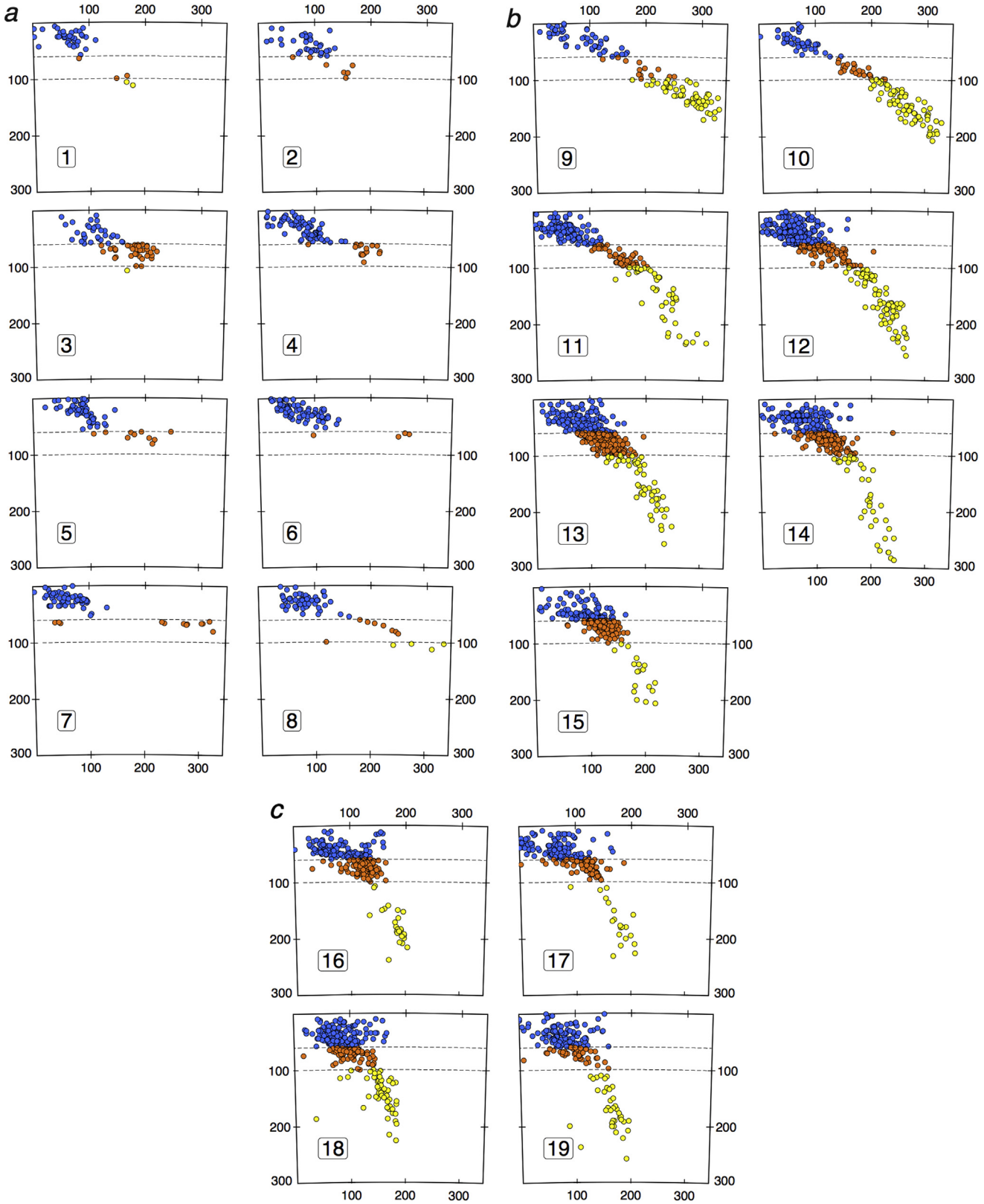

Fig. 4. Hypocentral cross-sections. Depths are color-coded as in previous figures. Dashed lines indicate the 60-km and 100-km depths. Tick marks are at 100-km intervals, as shown on the sections. There is no vertical exaggeration and Earth's curvature is taken into account. Number of sections refers to location on Fig. 3. (For interpretation of the references to color in this figure legend, the reader is referred to the web version of this article.)

Please cite this article in press as: Guzmán-Speziale, M., Zúñiga, F.R., Differences and similarities in the Cocos–North America and Cocos–Caribbean convergence, as revealed by seismic moment tensors, Journal of South American Earth Sciences (2015), http://dx.doi.org/10.1016/j.jsames.2015.10.002

displacement takes place during an earthquake. It may be calculated from the **T** and **P** axes by (e.g., Jost and Herrmann, 1989):

$$\mathbf{U} = \frac{1}{\sqrt{2}}(\mathbf{T} + \mathbf{P}) \quad (3)$$

The horizontal component of the slip vector of thrust-faulting earthquakes along convergent plate margins should point towards the azimuth of plate convergence (e.g., McCaffrey, 1992). In fact, many directions of plate convergence were originally obtained in this manner (e.g., DeMets et al., 1990), although sometimes this azimuth deviates from direction of plate in what is termed *oblique plate convergence*, in such cases where strain partitioning takes place (e.g., Fitch, 1972; McCaffrey, 1992, 1994).

Techniques independent of earthquake parameters (Global Positioning, for example) are now used to calculate relative plate motions (e.g., DeMets et al., 2010). Here, we use horizontal components of slip vectors along both margins to compare to the direction of plate convergence determined with independent parameters, as given in DeMets et al. (2010).

5. Results

There are 3552 events in our *EHB-ISC* catalog which meet the criteria set forth above for events related to the convergence process. An epicentral map is presented in Fig. 2, together with graphs showing events as a function of longitude and magnitude. Table 1 shows number of events for each convergence realm, sorted by depth and magnitude.

Only 15% of the events reported in *EHB-ISC* are related to Coco–Noam convergence. That is, 542 out of 3552 total. The other 3010 belong to Coco–Carb convergence. The number of interplate events (those with depths of 60 km or less) is also significantly smaller along Coco–Noam (444) than along Coco–Carb (1470). A similar situation takes place in the transition zone (60–100 km depth), with 95 events vs. 1046 (8% in Coco–Noam, of the total 1141 events). Within the subducted slab ($z > 100$ km) there are practically no events for Coco–Noam (only three), and 494 for Coco–Carb (Fig. 2; Table 1). In terms of magnitude, larger earthquakes occur along the Coco–Noam margin: two events with magnitude 8.0 or greater, as opposed to none along Coco–Carb; and 12 earthquakes with magnitudes between 7.0 and 8.0 for the former, compared to 9 for the latter. For smaller magnitudes, the trend is reversed. For example, for magnitudes smaller than 5.0, there are 270 events along Coco–Noam (221 shallow, 47 intermediate, and 2 deep), compared to 2169 along Coco–Carb (1052 shallow, 743 intermediate, and 374 deep) (Fig. 2; Table 1).

Using data from the *EHB-ISC* catalog we have been able to shed some light into the geometry of the subducted Cocos plate. We have done so by obtaining seismic cross-sections (Figs. 3 and 4) and adjusting a surface to the hypocenters (Fig. 5). In general, the dip shoals from NW to SE, as the Cocos plate is being subducted underneath the North America plate, from longitude 105° to −96°. In fact, in Central Mexico the *Wadati-Benioff zone* is no deeper than 100 km (cross-sections 2 through 7, Figs. 3 and 4). On the other hand, the dip of subduction is fairly constant underneath Caribbean, form latitude −96° to −85°, and hypocenters are located to depths close to 300 km (cross-sections 11 to 19, Figs. 3 and 4). The surface fitted to hypocentral locations (Fig. 5) shows essentially the same results as the seismic cross-sections: a shoaling, from NW to SE, of the dip of subduction underneath the North America plate, and a sudden deepening underneath the Caribbean, east of longitude −96°.

There are a total of 943 normal- or thrust-faulting solutions in our *CMT* compilation. Of these, 240 belong to Coco–Noam, and 703 to Coco–Carb. Sorted by type of faulting, there are 194 thrust-faulting mechanisms (192 shallow, and two intermediate; none deep) along the Cocos–North America plate margin, and 474 (326 shallow, 108 intermediate, and 40 deep) along Coco–Carb. As for normal-faulting solutions, 46 belong to Coco–Noam (14 shallow, 32 intermediate, none deep), and 229 to Coco–Carb (92 shallow, 96 intermediate, 41 deep) (Fig. 6; Table 2).

The convergent margin, that is, the length of the Middle America trench along Coco–Noam is 1024 km, and 1423 km along Coco–Carb. From the results presented in Table 2, along Coco–Noam there is one shallow, thrust-faulting event approximately every 5 km; for Coco–Carb there is one every 3 km.

The sum of scalar seismic moment for shallow, thrust-faulting mechanisms is about three times along Coco–Noam than along Coco–Carb. Shallow events contribute to most of the sum of seismic moment along both margins: $4.206 \cdot 10^{21}$ N m along Coco–Noam, and $1.390 \cdot 10^{21}$ N m along Coco–Carb (Fig. 7; Table 3). The sum of seismic moment for shallow normal-faulting events along Coco–Noam is about half of that along Coco–Carb ($2.452 \cdot 10^{20}$ N m versus $5.269 \cdot 10^{20}$ N m) while for intermediate-depth events, it is about the same ($1.154 \cdot 10^{20}$ N m compared to $1.795 \cdot 10^{20}$ N m) (Fig. 7; Table 3).

We also calculated average seismic moment per event, again by margin, depth, and type of faulting (Table 3). Shallow, thrust-faulting events along Coco–Noam have the largest average per event of all, $2.191 \cdot 10^{19}$ N m about one order of magnitude larger than those along Coco–Carb (Fig. 7; Table 3). The scalar seismic moment divided by the length of the convergent margin is $4.108 \cdot 10^{18}$ N m/km for thrust-faulting earthquakes, $2.395 \cdot 10^{17}$ N m/km for normal-faulting *CMTs* along Coco–Noam, while $9.770 \cdot 10^{17}$ N m/km and $3.703 \cdot 10^{17}$ N m/km for thrust- and normal-faulting events along Coco–Carb.

There is a noticeable difference in **P**-axis azimuth for shallow, thrust-faulting earthquakes, between the two convergent margins. Average for Coco–Noam is 20.1° (15° standard deviation), whereas for Coco–Carb the average is 29.4°, with a standard deviation of 10.1° (Fig. 8). The azimuth of plate convergence Coco–Noam (31.6°) falls within one standard deviation of azimuth of **P** axes. On the other hand, Coco–Carb convergence (20.3°) is about one standard deviation from average (Fig. 8).

The azimuth of **T** axes of intermediate and deep ($z > 60$ km), normal-faulting events as well as deep thrust-faulting events is oriented, in general, in the direction of maximum dip of the subducted slab (Fig. 9): Underneath the North America plate the azimuth gradually increases from about −10° to some 30°; on the Caribbean side, the azimuth goes from 60°–70° on the western side, to about 45° in the East.

Plunge of **T** axes of intermediate-depth events show a maximum of about 30° for the subducted Cocos plate underneath North America (Fig. 9). There are no thrust-faulting events deeper than 60 km on Coco–Noam, except for the two isolated events near the western edge of the region under dconsideration (Fig. 6). Plunge of

Table 1
Events from the hipopcentral catalog, sorted by depth and magnitude.

	Coco − Noam				Coco − Carb				Sum
	A	B	C	All	A	B	C	All	
$M \geq 8.0$	2	0	0	2	0	0	0	0	2
$7.0 \leq M < 8.0$	10	2	0	12	7	1	1	9	21
$6.0 \leq M < 7.0$	25	5	0	30	45	29	15	89	119
$5.0 \leq M < 6.0$	186	41	1	228	366	273	104	743	971
$4.0 \leq M < 5.0$	221	47	2	270	1052	743	374	2169	2439
Total	444	95	3		1470	1046	494		
Grand total				542				3010	3552

A. $z \leq 60$ km; B. $60 < z \leq 100$ km; C. $z > 100$ km.

Please cite this article in press as: Guzmán-Speziale, M., Zúñiga, F.R., Differences and similarities in the Cocos–North America and Cocos–Caribbean convergence, as revealed by seismic moment tensors, Journal of South American Earth Sciences (2015), http://dx.doi.org/10.1016/j.jsames.2015.10.002

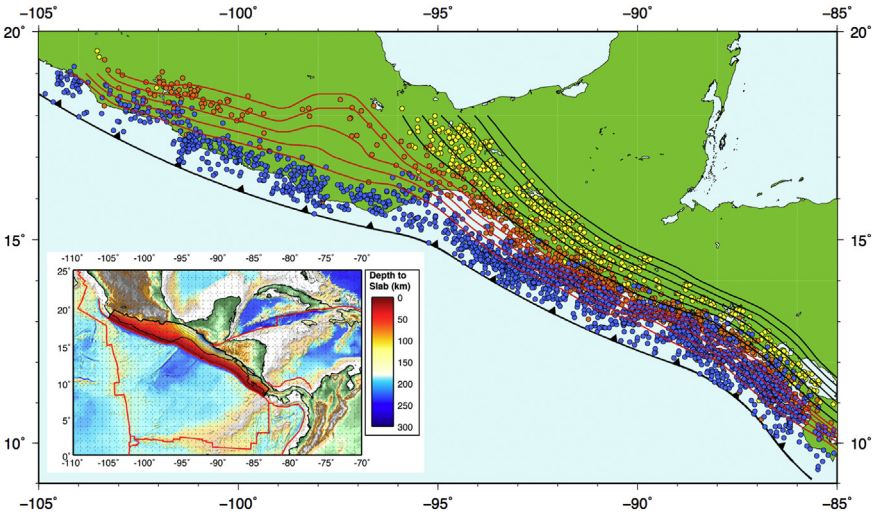

Fig. 5. Contoured surface for the subducted Cocos plate. Red lines are at 10-km intervals, from 40 km to 80 km. Black lines are at 25-km intervals, from 100 to 225 km. Inset shows the model for the subducted Cocos plate obtained in *Slab1.0* by Hayes et al. (2012). (For interpretation of the references to color in this figure legend, the reader is referred to the web version of this article.)

T axes in Coco–Carb range from 0° to 90°, 0° to 45° corresponding, by definition (see above), to normal-faulting events, and 45° to 90 to thrust-faulting earthquakes.

We found that *CLVD* ratio for shallow, thrust-faulting earthquakes is a function of scalar seismic moment: at lower scalar seismic moments (and hence magnitudes), ratio is higher (Fig. 10). In terms of percentage, *CLVD* ratio for shallow, trhust faulting earthquakes is essentially the same for both margins: about 92% of the events have f_{clvd} of 0.2 or less, with two thirds of the events found in the 0.0 to 0.1 range (Fig. 10).

Horizontal component of earthquake slip vectors have an average of 24.3° along Coco–Noam (standard deviation 16.6°), whereas the average along Coco–Carb is 33.2°, with a standard deviation of 12.4° (Fig. 11). Average direction of relative plate motion is 24° and 32°, respectively.

6. Discussion

From results presented here, there is a clear difference in many seismic parameters between Cocos–North America and Cocos–Caribbean convergence at the proposed limit between the two convergent margins, longitude −96°.

In terms of number of events (Table 1), most of the activity takes place along the Coco–Carb margin. In fact, there is practically no seismicity deeper than 100 km underneath the North America plate, except for three events west of longitude −102° (Fig. 2). On the other hand, magnitudes are larger along Coco–Noam, particularly at shallow depths (Table 1; Fig. 2). What is the meaning of this difference? Several authors (e.g., Uyeda and Kanamori, 1979; Uyeda, 1982; Pacheco et al., 1993; Guzmán-Speziale and Gómez González, 2006) have proposed that coupling is stronger along the Coco–Noam than along Coco–Carb margin. Pacheco et al. (1993) calculated a *seismic coupling coefficient* of 0.26 for Coco–Noam, and 0.05 for Coco–Carb while Guzmán-Speziale and Gómez-González (2006) showed that seismic strain rate along the former is one order of magnitude larger ($2.8 \cdot 10^{-7}\ yr^{-1}$ vs. $3.7 \cdot 10^{-8}\ yr^{-1}$) for a 27-year period. Our results suggest that coupling between the Coco–Noam is higher because the subducting slab is flatter. Consequently, the interface is larger and then opposes more resistance to gravity forces. Therefore, more elastic strain has to be accumulated to be released in less frequent but larger earthquakes. The change in coupling probably takes place gradually, over an extended area, as suggested by Franco et al. (2012).

We have determined an up-to-date geometric model of the subducted Cocos plate using the hypocenters from our improved *EHB-ISC* catalog. First, a close, step-by-step look from northwest to southeast is provided by 19 adjacent seismic cross-sections located perpendicular to the trench (Figs. 3 and 4). Second, a surface is adjusted to the hypocenters (Fig. 5). To our knowledge, the only recent model for the entire subducted Cocos plate is that of Hayes et al. (2012) (see Fig. 5). These authors determined the three-dimensional geometry of most subduction zones gobally. Previous models for the entire Cocos plate were those of Bevis and Isacks (1984) and Burbach et al. (1984). Local or regional models have also been obtained throughout the years (e.g., Molnar and Sykes, 1969; Hanus and Vanek, 1978; Bevis and Isacks, 1984; Burbach et al., 1984; Protti and McNally, 1994; Arzate et al., 1995; Pardo and Suárez, 1995; García Quintero, 2007; Pérez-Campos et al., 2008; Melgar and Pérez-Campos, 2011).

Our model confirms and improves on all these models, particularly on that of Hayes et al. (2012): The subducted Cocos plate underneath the North America plate changes dip along the 1024 km of trench which comprises the plate boundary, from steeply dipping (about 45°) in the northwest, to almost flat subduction around longitude −99°, staying flat to abouut −96°. On the other hand, it dips rather consistently (40° to 50°) underneath the Caribbean plate (Figs. 4 and 5). Our results also show that the subducted Cocos plate is warped at longitudes −99° to −96° (Fig. 5), forming a *bulge*. It could be argued that the bulge is an artifact of the adjusting algorithm, particulary because seismicity is not abundant in the area. However, azimuth of **T** axes from regional *CMT*s are oriented perpendicular to the isodepth lines, suggesting tension in the direction of maximum dip, and consequently the very existence of the bulge (see below). We suggest this warping is a geometric response of the subducted slab to a gradual and smooth change in dip. Our results, on the other hand, cannot fully resolve a long-standing controversy: whether the change of dip within the subducted slab is due to a smooth transition or to a tear within the subducted slab, although. We favor a continuous model because the lines of equal depth (Fig. 5) do not show a break or tear, at the scale shown. The model presented herein shows the geometry of the

Please cite this article in press as: Guzmán-Speziale, M., Zúñiga, F.R., Differences and similarities in the Cocos–North America and Cocos–Caribbean convergence, as revealed by seismic moment tensors, Journal of South American Earth Sciences (2015), http://dx.doi.org/10.1016/j.jsames.2015.10.002

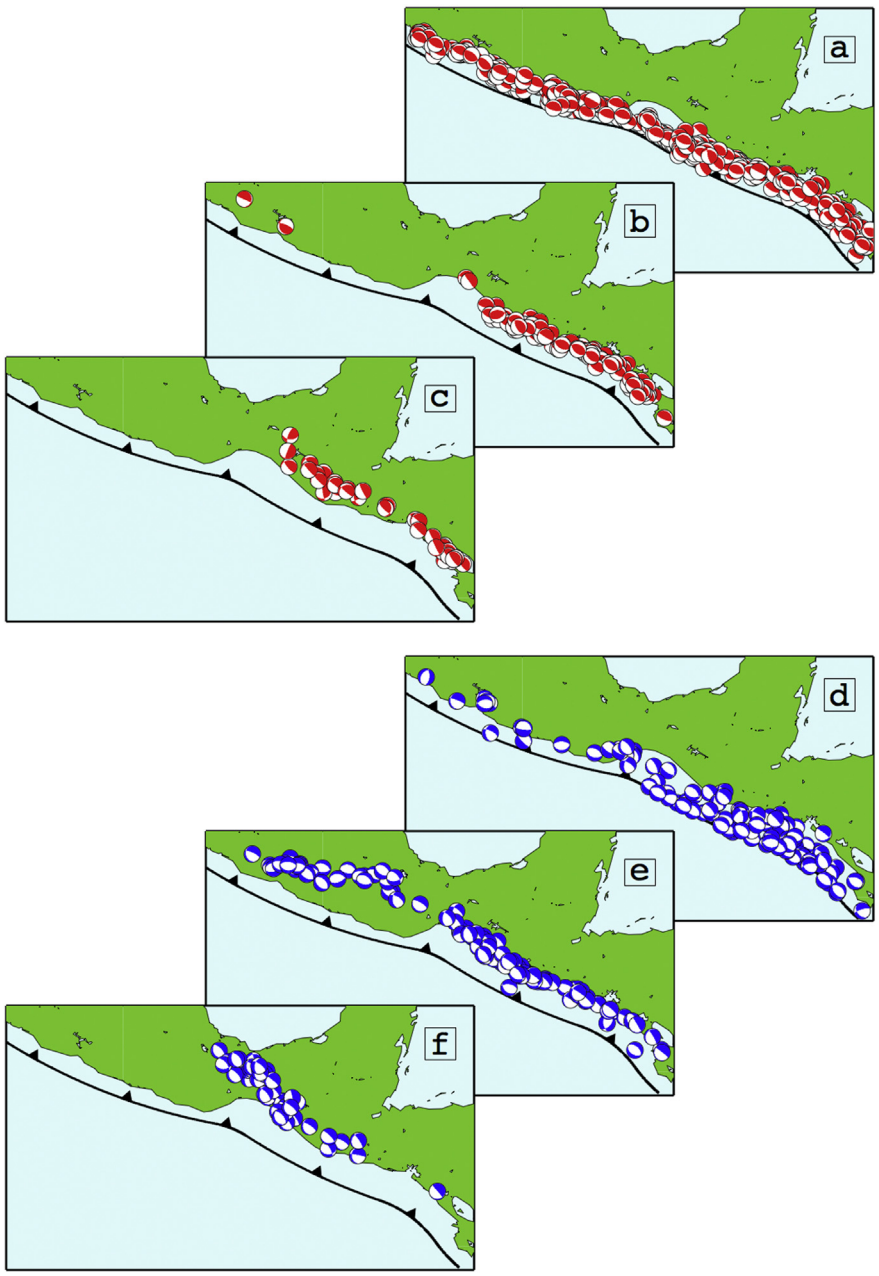

Fig. 6. Earthquake fault-plane solutions from *CMT* data. a. Shallow ($z \leq 60$ km), thrust-faulting mechanisms. b. Intermediate-depth ($60 < z \leq 100$ km) thrust-faulting events. c. Deep ($z > 100$ km), thrust-faulting earthquakes. d. to f. Normal-faulting events, in same layout as for thrust-faulting events.

Table 2
Number of *CMTs* by depth and type of faulting.

	Coco – Noam		Coco – Carb	
	Thrust	Normal	Thrust	Normal
$z \leq 60$	192	14	326	92
$60 < z \leq 100$	2	32	108	96
$z > 100$	0	0	40	41
Total	194	46	474	229
Sum	240		703	

subducted Cocos plate in more detail than in Hayes et al. (2012) because, aside from fitting a surface to the hypocentral data as both Hayes et al. (2012) and us do, we also obtain non-overlapping cross-sections which allows to see the transition from shallow-dipping to steeply dipping subducted slab in detail. Furthermore, we have been able to uncover a probable bulge within the slab.

From the *CMT* catalog, we see that shallow ($z \leq 60$ km), thrust-faulting earthquakes occur along the entire margin (Table 2; Figs. 6 and 8). Cleraly, these earthquakes are associated to the convergence process. We found out that thrust-faulting mechanisms extend to a maximum depth of 60 km along the Coco–Noam margin, so we tentatively propose this as the lower-depth transition (cf., Pacheco et al., 1993). On the other hand, shallow ($z < 60$ km), normal-faulting events are abundant along Coco–Carb but not along Coco–Noam (Fig. 6). Bending (flexural) stresses must be larger at Coco–Carb because of the larger dip of subduction.

Total number of thrust-faulting events along Coco–Noam is almost half of the ones along Coco–Carb (Table 2), but scalar seismic moment is higher along the former, whether considered as

Please cite this article in press as: Guzmán-Speziale, M., Zúñiga, F.R., Differences and similarities in the Cocos–North America and Cocos–Caribbean convergence, as revealed by seismic moment tensors, Journal of South American Earth Sciences (2015), http://dx.doi.org/10.1016/j.jsames.2015.10.002

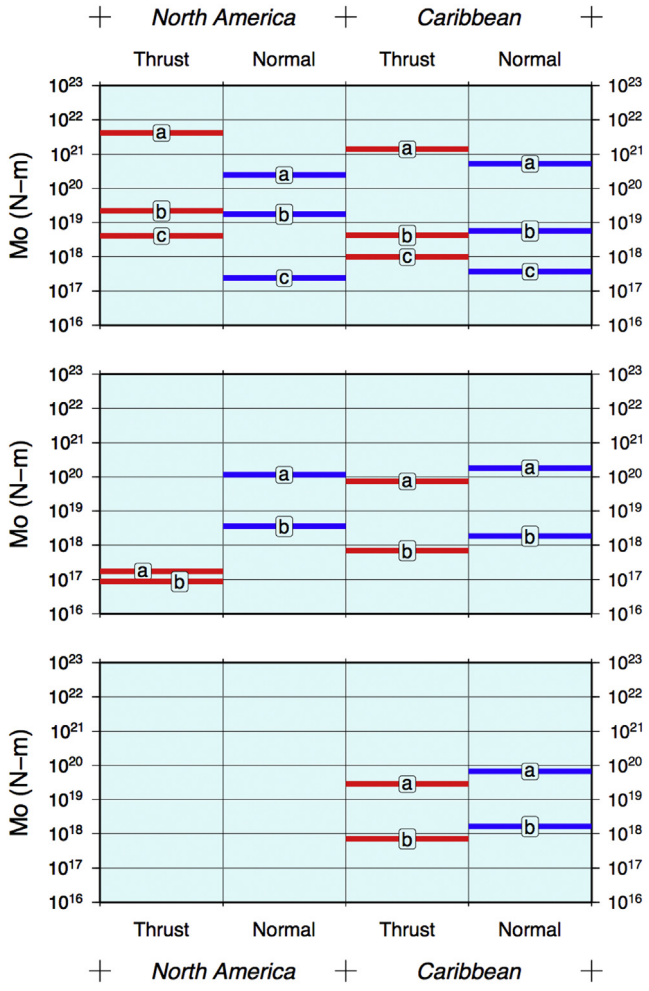

Fig. 7. Cummulative scalar seismic moment (in N·m) for shallow (top panel), intermediate-depth (middle), and deep events (bottom). Red lines correspond to trhust-faulting mechanisms, blue lines to normal-faulting events. a is total moment; b is average per event, and c, average per kilometer of margin. (For interpretation of the references to color in this figure legend, the reader is referred to the web version of this article.)

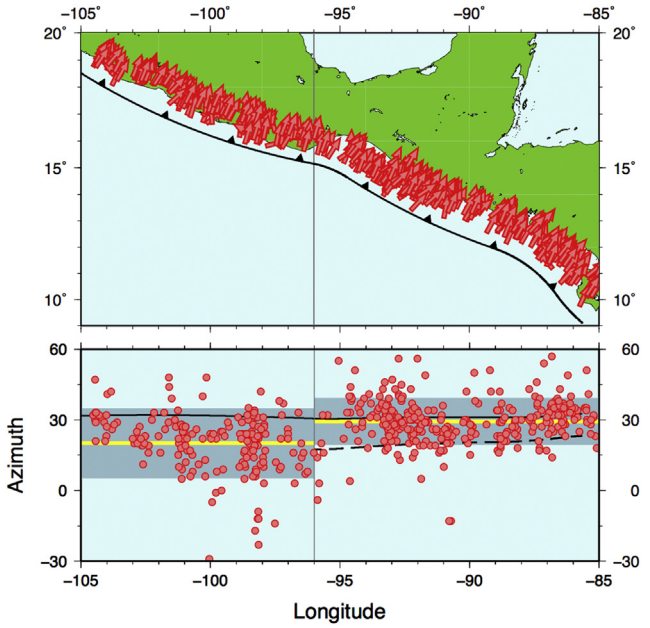

Fig. 8. Horizontal component of **P** axes for shallow, thrust-faulting earthquakes ($z \leq 60$ km). Top. Map view. Bottom, as a function of longitude. Yellow line is mean; gray area represents ± one standard deviation. Both mean and standard deviation separated by Coco–Noam and Coco–Carb convergence. Solid black line on both sides is azimuth of Coco–Noam convergence; dashed line, azimuth of Coco–Carb convergence. (For interpretation of the references to color in this figure legend, the reader is referred to the web version of this article.)

plate (e.g., Harlow and White, 1985; DeMets, 2001; Lyon-Caen et al., 2006; LaFemina et al., 2009; Franco et al., 2012). A combination of both factors is also a possibility. Oblique plate convergence probably does not play a major role because the angle of obliquity along the margin is very small (3° in some cases) (Guzmán-Speziale and Gómez, 2002).

The azimuth (horizontal component) of **P** axes is clearly different on both margins (Fig. 8), which we interpret as a differentiated state of stress. Again, relative and/or absolute plate motion may be responsible.

Table 3
Scalar seismic moment, in N m.

	Coco − Noam				Coco − Carb			
	Thrust		Normal		Thrust		Normal	
	Sum	Per event[a]	Sum	Per event[a]	Sum	Per event[a]	Sum	Per event[a]
$z \leq 60$	4.206×10^{21}	2.191×10^{19}	2.452×10^{20}	1.752×10^{19}	1.390×10^{21}	4.265×10^{18}	5.269×10^{20}	5.727×10^{18}
$60 < z \leq 100$	1.746×10^{17}	8.730×10^{16}	1.154×10^{20}	3.607×10^{18}	7.502×10^{19}	6.946×10^{17}	1.795×10^{20}	1.870×10^{18}
$z > 100$	0	0	0	0	2.872×10^{19}	7.179×10^{17}	6.706×10^{19}	1.636×10^{18}
Total	4.207×10^{21}	2.191×10^{19}	3.606×10^{20}	2.112×10^{19}	1.494×10^{21}	5.678×10^{18}	7.734×10^{20}	9.232×10^{18}

[a] Average per event.

a sum, as an average per event, or as an average per kilometer of plate boundary (Fig. 7; Table 3). Once again, this result suggests that coupling along the Coco–Noam is stronger than along the Coco–Carb. This could be a consequence of the motion of the plates: in an absolute reference frame, the North America plate is advancing towards the subducting Cocos plate, whereas the Caribbean plate is stationary or slowly retreating from the Cocos plate (see above). Or, it could be a consequence of the Central America forearc sliver being dettached from the nuclear Caribbean

Horizontal component of **T** axes of both normal-faulting ($z > 60$ km), and thrust-faulting ($z > 100$ km) earthquakes show that at intermediate and deep depths, tension (least compression) takes place in the direction of the maximum dip of the subducted slab. This includes the area of the bulge discussed above, where directions of **T** axes wrap around the contours of equal depth of the subducted slab (Fig. 9). This suggests that the bulge does exist and it is not an artifact of the fitting of the surface to the observed hypocentral data.

Please cite this article in press as: Guzmán-Speziale, M., Zúñiga, F.R., Differences and similarities in the Cocos–North America and Cocos–Caribbean convergence, as revealed by seismic moment tensors, Journal of South American Earth Sciences (2015), http://dx.doi.org/10.1016/j.jsames.2015.10.002

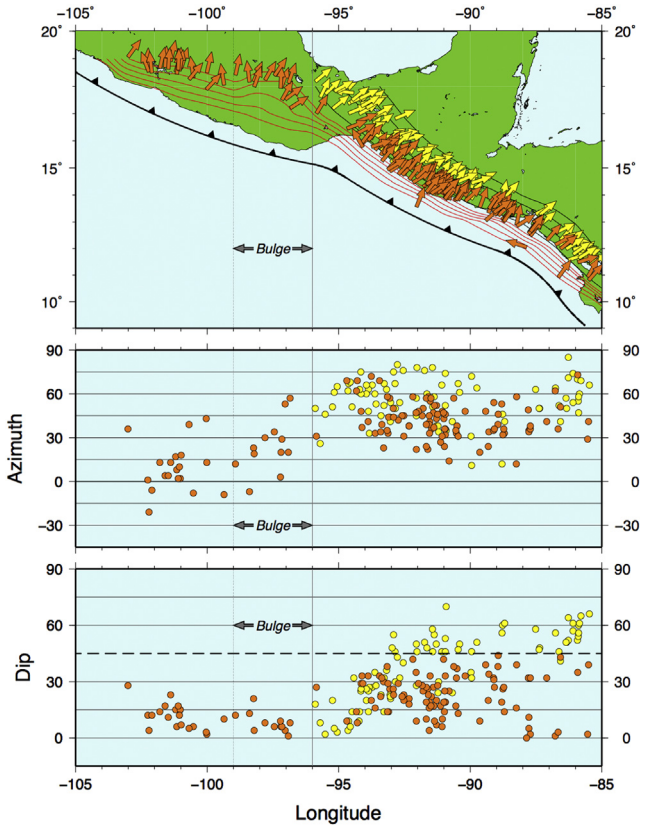

Fig. 9. Azimuth of **T** axes for intermediate-depth and deep ($z > 60$ km), normal-faulting earthquakes (orange arrows and dots), and deep ($z > 100$ km), thrust-faulting events (yellow). Top. Map view. Bottom, as a function of longitude. Location of proposed *bulge"* is indicated. (For interpretation of the references to color in this figure legend, the reader is referred to the web version of this article.)

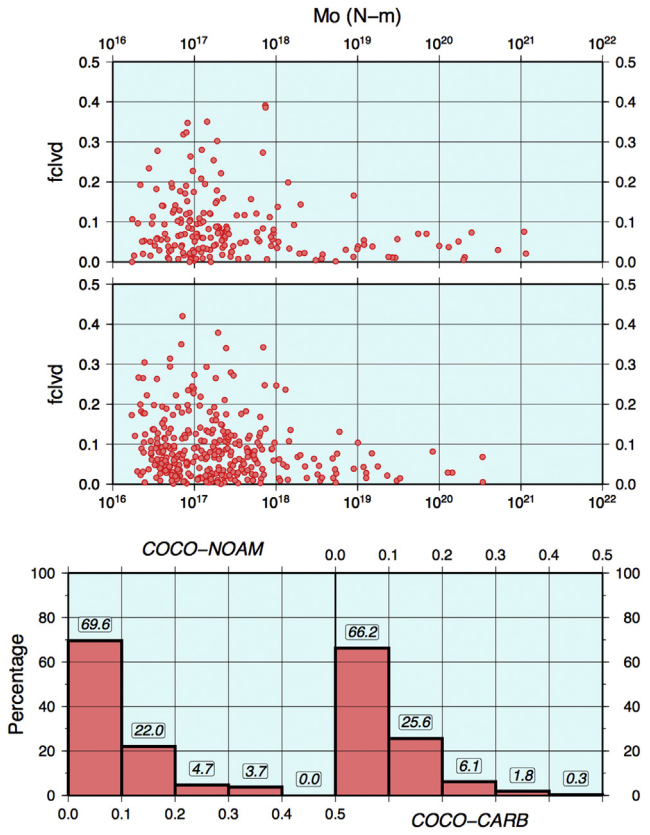

Fig. 10. *CLVD* ratio for shallow, thrust-faulting events from the CMT catalog. Top: *CLVD* ratio as a function of scalar seismic Moment M_0 for Cocos–North America convergence. Middle: Same as previous, but for Cocos–Caribbean convergence. Bottom: histogram of percentage in 0.1 ratio intervals, for Coco–Noam (left), and Coco–Carb (right).

Dip of **T** axes reflects dip of subduction: along Cocos–Noam, where the dip is shallow (Figs. 4 and 5), plunge of **T** axes is less than 30° west of −100° longitude, and even shallower (less than 15°) between −100° and −96° (Fig. 9), right where the apparent "bulge" in the subducted slab is located (Fig. 5). The shoaling of **T** axes suggests that the bulging is real. To the east of −96°, where the Cocos plate subducts underneath the Caribbean, plunge of **T** axes spans the entire range 0° to 90°. Evidently, this is translated into normal-faulting mechanisms if plunge is between 0° and 45°, whereas from 45° to 90° this will mean a thrust-faulting mechanism. A weaker coupling along the convergent margin (see above) may mean a stronger slab pull, as in the *Mariana type* of Uyeda (1982). This fact, together with a steeper angle of subduction, results in tensile (or least compressive) stresses plunging in a wide range of dips. Intermediate-depth (60 km $< z \leq$ 100 km) and deep ($z >$ 100 km) thrust-faulting earthquakes only occur in Caribbean side of the subducted slab because this is where the plunge of the **T** axes can exceed 45°.

CLVD ratios for shallow, thrust-faulting mechanisms along both margins show that are higher scalar seismic moments, the mechanism is closer to a double couple because the ratio is lower.Conversely, at lower magnitudes, focal mechanism has a larger *CLVD* component. This seems to be true similarly for both margins, with no discernible difference between them (Fig. 10). Nevertheless, in terms of percentage approximately two thirds of all mechanisms are close to having a pure double-couple mechanism, with a ratio of 0.1 or less (Fig. 10).

Azimuths of earthquake slip vectors for Coco–Noam (average 24°±17°) agree, within one standard deviation, with the average direction of plate convergence (32°), but azimuths along the Coco–Carb margin (32°±11°) do not (average convergence 20°). However, average azimuth along Coco–Carb (32°±11°) agrees very well with average direction of convergence Coco–Noam (calculated along the Coco–Carb margin) of 31° (Fig. 11). This result suggests that the Cocos plate east of −96° is in fact subducting only underneath the Central America forearc sliver, which is probably dettached from the Caribbean plate and attached to North America. Trend of **P** axes for shallow, thrust-faulting events (Fig. 8) shows a similar result. Where or how the attachment of the forearc sliver to North America is still the matter of study (e.g., Lyon-Caen et al., 2006; LaFemina et al., 2009; Franco et al., 2012) and complex issues need to be resolved, such as why there is abundant seismicity along the Central America Volcanic Arc (Cava) (e.g., Guzmán-Speziale et al., 2005) but not along the Tonalá fault in Chiapas (Fig. 1) (e.g., Guzmán-Speziale et al., 1989), or why motion along the Cava is right-lateral (e.g., Corti et al., 2005; Alonso-Henar et al., 2015), whereas it is left-lateral along the Tonalá fault (Fig. 1) (Molina-Garza et al. 2015). It is beyond the scope of this paper to try to shed light on them.

In general, there are significant differences in seismic parameters between Cocos–North America and Cocos–Caribbean convergence. Transition between the two convergence realms takes place at about longitude −96°, which suggests that this is the area of the change in overriding plate and hence the triple junction region. From a crustal point of view, it has not been possible to determine where the triple junction is (see above). Results presented here support the proposal presented by Guzmán-Speziale

Please cite this article in press as: Guzmán-Speziale, M., Zúñiga, F.R., Differences and similarities in the Cocos–North America and Cocos–Caribbean convergence, as revealed by seismic moment tensors, Journal of South American Earth Sciences (2015), http://dx.doi.org/10.1016/j.jsames.2015.10.002

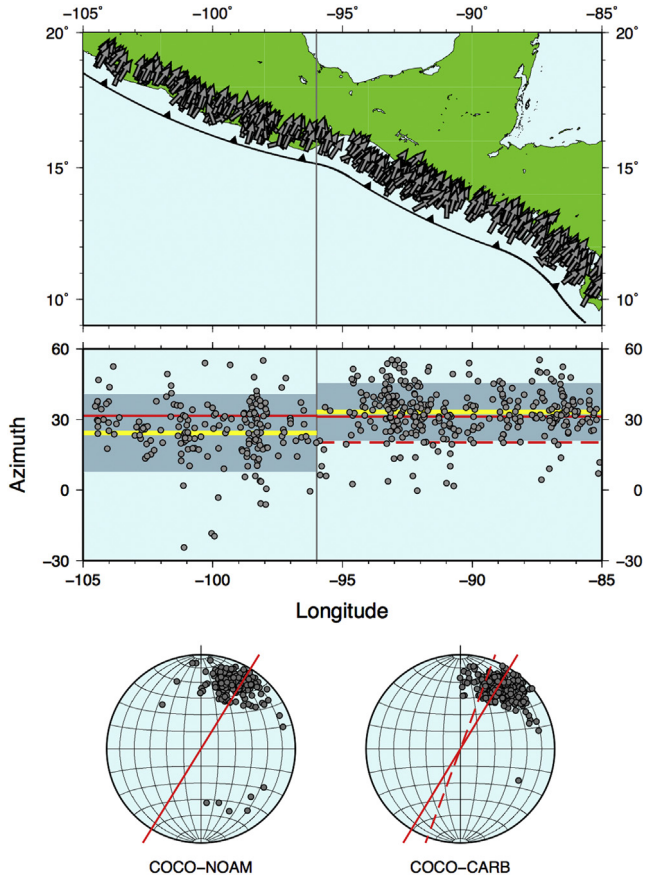

Fig. 11. Azimuth of earthquake slip vectors for shallow, thrust-faulting *CMT*'s. Top—map view. Middle-as a function of longitude. Yellow line is average; shaded area is ± one standard deviation; solid red line is average direction of Coco—Noam convergence; dashed red line is average direction of Coco—Carb plate convergence. Bottom— Stereographic projection of slip vectors azimuths for Coco—Noam (left) and Coco—Carb (right) convergence; solid red line is average direction of Coco—Noam convergence; dashed red line is average direction of Coco—Carb plate convergence. (For interpretation of the references to color in this figure legend, the reader is referred to the web version of this article.)

and coworkers (e.g., Guzmán-Speziale et al., 1989; Guzmán-Speziale and Meneses Rocha, 2000) that the triple junction is an area of deformation that spans the state of Chiapas, from Guatemala to the isthmus of Tehuantepec (Fig. 1), coinciding with changes found in this work.

Most of the differences found in this work and results from previous authors tend to confirm the existence of two different modes of subduction along the Middle America trench: *Chilean* along the Cocos—North America interface, and *Mariana* along Cocos—Caribbean. Many authors (e.g., Harlow and White, 1985; DeMets, 2001; Corti et al., 2005; Guzmán-Speziale and Gómez-González, 2006; Correa-Mora et al., 2009; LaFemina et al., 2009; Alvarado et al., 2011) have proposed that the Central America forearc sliver may be partially or fully dettached from the Caribbean plate along the Central America volcanic arc. Consequently, seismicity along the Middle America trench may not reflect convergence of Cocos and Caribbean plates directly. Instead, it may reflect partitioning, although the issues of the Tonalá fault having an opposite sense of motion (Fig. 1) and the small angle of obliquity (see above) are yet to be resolved.

There is still debate as to whether the overriding plate changes from North America to Caribbean at longitude −96°. Whether or not this is the case, there are definitely many changes in the tectonics and geomorphology at this location, as pointed out above. Results presented here point to a clear change in several seismic parameters precisely at this location, and continuity northward and southward of here. Perhaps then, instead of stating that we found changes in seismic parameters associated to a change in overriding plate, we may indirectly infer this change from North America to Caribbean plates precisely from the remarkable differences in earthquake parameters.

7. Conclusions

In summary, the following seismic differences between Cocos—North America and Cocos—Caribbean convergence were found:

1. Significant changes take place around the −96° longitude.
2. There are less earthquakes along the Coco—Noam margin than along Coco—Carb, but magnitudes are larger.
3. A different dip of subduction is evident: shallow along Coco—Noam, and deep along Coco—Carb. Transition between the two takes place smoothly in the form of a warp or bulge in the subducted plate.
4. There are more events, either normal- or thrust-faulting, along Coco—Carb than along Coco—Noam.
5. Sum of scalar seismic moment for shallow, thrust-faulting events is about four times larger along Coco—Noam. Trend is reversed for normal-faulting or deeper events.
6. Shallow, normal-faulting events are more abundant along Coco—Carb, due perhaps to flexural stresses and low seismic coupling
7. Azimuth of **T** axes for intermediate- and deep events follow the direction of maximum dip within the subducted plate.
8. *CLVD* ratio is not different from one convergent margin to the other, but it is a function of earthquake size.
9. Horizontal component of shallow earthquake slip vectors follow the direction of relative Coco—Noam motion, on both margins.
10. Detachment of the Central America forearc sliver may also contribute to observed differences.

Acknowledgments

We are grateful to two anonymous reviewers for their constructive comments and criticisms. We also thank Franck Audemard, Regional Editor of the Journal, for his careful and meticulous review of the latter version of the manuscript. Support for this work came from *Consejo Nacional de Ciencia y Tecnología* (Mexico) grant 58453-T, and from Universidad Nacional Autónoma de México, through grant *Papiit* IN113210. Centro de Geociencias contribution number 1345.

References

Alonso-Henar, J., Schreurs, G., Martínez-Díaz, J.J., Álvarez-Gómez, J.A., Villamor, P., 2015. Neotectonic development of the El Salvador Fault Zone and implication for the deformation in the Central America volcanic arc. Insights for 4D analogue experiments. Tectonics. http://dx.doi.org/10.1002/2014TC003723.

Alvarado, D., DeMets, C., Tikoff, B., Hernández, D., Wawrzyniec, T.F., Pullinger, C., Mattioli, G., Turner, H.L., Rodríguez, M., Correa-Mora, F., 2011. Forearc motion and deformation between El Salvador and Nicaragua: GPS, seismic, structural, and paleomagnetic observations. Lithosphere 3, 3–21.

Argus, D., Gordon, R.G., DeMets, C., 2011. Geologically current motion of 56 plates relatively to the no-net-rotation reference frame. Geochem. Geophys. Geosyst. 12, Q11001. http://dx.doi.org/10.1029/2011GC003751.

Arzate, J.A., Marechal, M., Urrutia-Fucugauchi, J., 1993. A preliminary crustal model of the Oaxaca continental margin and subduction zone from magnetotelluric and gravity mesurements. Geofís. Int. 32, 441–452.

Arzate, J.A., Marechal, M., Livelybrooks, D., 1995. Electrical image of the subducting Cocos plate from magnetotelluric observations. Geology 23, 703–706.

Becker, T.W., Schaeffer, A.J., Lebedev, S., Conrad, C.P., 2015. Toward a generalized

plate motion reference frame. Geophys. Res. Lett. 42, 3188–3196. http://dx.doi.org/10.1002/2015GL063695.
Bevis, M., Isacks, B.L., 1984. Hypocentral trend surface analysis: proving the geometry of Benioff zones. J. Geophys. Res. 89, 6153–6170.
Bird, P., 2003. An updated digital model of plate boundaries. Geochem. Geophys. Geosyst. 4, 1027. http://dx.doi.org/10.1029/2001GC000252.
Burbach, G.V., Frohlich, C., Pennington, W.D., Matumoto, T., 1984. Seismicity and tectonics of the subducted Cocos plate. J. Geophys. Res. 89, 7719–7735.
Burkart, B., 1978. Offset across the Polochic fault of Guatemala and Chiapas, Mexico. Geology 6, 328–332.
Burkart, B., 1983. Neogene North American – Caribbean plate boundary across northern Central America: offset along the polochic fault. Tectonophysics 99, 251–270.
Cáceres, D., Monterroso, D., Tavakoli, B., 2005. Crustal deformation in northern Central America. Tectonophysics 404, 119–131.
Campos-Enríquez, J.O., Sánchez-Zamora, O., 2000. Crustal structure across southern Mexico inferred from gravity data. J. S. Am. Earth Sci. 13, 479–489.
Chael, E., Stewart, G.S., 1982. Recent large earthquakes along the middle America trench and their implications for the subduction process. J. Geophys. Res. 87, 329–338.
Chen, T., Clayton, R.W., 2012. Structure of central and southern Mexico from velocity and attenuation tomography. J. Geophys. Res. 117, B09302. http://dx.doi.org/10.1029/2012JB009233.
Correa-Mora, F., DeMets, C., Alvarado, D., Turner, H.L., Mattioli, G., Hernández, D., Pullinger, C., Rodríguez, M., Tenorio, C., 2009. GPS-derived coupling estimates for the Central America subduction zone and volcanic arc faults: El Salvador, Honduras and Nicaragua. Geophys. J. Int. 179, 1279–1291.
Corti, G., Carminati, E., Mazzarini, F., Garcia, M.O., 2005. Active strike-slip faulting in El Salvador, Central America. Geology 33, 989–992.
Cruz-Atienza, V.M., Husker, A., Legrand, D., Caballero, E., Kostoglodov, V., 2015. Nonvolcanic tremor locations and mechanisms in Guerrero, Mexico, from energy-based and particle motion polarization analysis. J. Geophys. Res. 120, 275–289. http://dx.doi.org/10.1002/2014JB011389.
DeMets, C., 2001. A new estimate for present-day Cocos–Caribbean plate motion: implications for slip along the Central American volcanic arc. Geophys. Res. Lett. 28, 4043–4046.
DeMets, C., Gordon, R.G., Argus, D.F., Stein, S., 1990. Current plate motions. Geophys. J. Int. 101, 425–478.
DeMets, C., Jansma, P.E., Mattioli, G.S., Dixon, T.H., Farina, F., Bilham, R., Calais, E., Mann, P., 2000. GPS geodetic constraints on Caribbean–North America plate motion. Geophys. Res. Lett. 27, 437–440.
DeMets, C., Mattioli, G., Jansma, P., Rogers, R.D., Tenorio, C., Turner, H.L., 2007. Present motion and deformation of the Caribbean plate: constraints from new GPS geodetic measurements from Honduras and Nicaragua. In: Mann, P. (Ed.), Geologic and Tectonic Development of the Caribbean Plate Boundary in Northern Central America, Geological Society of America Special Paper, vol. 428, pp. 21–36. http://dx.doi.org/10.1130/2007.2428(02).
DeMets, C., Gordon, R.G., Argus, D.F., 2010. Geologically current plate motions. Geophys. J. Int. 181, 1–80.
Dougherty, S.L., Clayton, R.W., Helmberger, D.V., 2012. Seismic structure in central Mexico: implications for fragmentation of the subducted Cocos plate. J. Geophys. Res. 117, B09316. http://dx.doi.org/10.1029/2012JB009528.
Dziewonski, A.M., Chou, T.A., Woodhouse, J.H., 1981. Determination of earthquake source parameters from waveform data for studies of global and regional seismicity. J. Geophys. Res. 86, 2825–2852.
Dziewonski, A.M., Woodhouse, J.H., 1983. An experiment in systematic study of global seismicity: centroid-moment tensor solutions for 201 moderate and large earthquakes of 1981. J. Geophys. Res. 88, 3247–3271.
Ekström, G., Nettles, M., Dziewonski, A.M., 2012. The global CMT project 2004–2010: centroid-moment tensors for 13,017 earthquakes. Phys. Earth Planet. Inter. 200–201, 1–9. http://dx.doi.org/10.1016/j.pepi.2012.04.002.
Engdahl, E.R., van der Hilst, R., Buland, R., 1998. Global teleseismic earthquake relocation with improved travel times and procedures for depth determination. Bull. Seismol. Soc. Am. 88, 722–743.
Fitch, T.J., 1972. Plate convergence, transcurrent faults and internal deformation adjacent to Southeast Asia and the Western Pacific. J. Geophys. Res. 77, 4432–4460.
Franco, A., Laserre, C., Lyon-Caen, H., Kostoglodov, V., Molina, E., Guzmán-Speziale, M., Monterosso, D., Robles, V., Figueroa, C., Amaya, W., Barrier, E., Chiquin, L., Moran, S., Flores, O., Romero, J., Santiago, J.A., Manea, M., Manea, V.C., 2012. Fault kinematics in northern Central America and coupling along the subduction interface of the Cocos plate, from GPS data in Chiapas (Mexico), Guatemala and El Salvador. Geophys. J. Int. 189, 1223–1236.
Frohlich, C., Apperson, K.D., 1992. Earthquake focal mechanisms, moment tensors, and the consistency of seismic activity near plate boundaries. Tectonics 11, 279–296.
García-Quintero, J.J., 2007. Geometría, sismicidad y deformación de la placa de Cocos subducida. M. Sc. thesis. UNAM, p. 42.
Geolimex Working Group, 1994. Reflections from the subducting plate? First results of a Mexican traverse. Zentralblatt Geol. Palaontologie Teil I 1/2, 541–553. Stuttgart.
Gorbatov, A., Fukao, Y., 2005. Tomographic search for missing link between the ancient Farallon subduction and the present Cocos subduction. Geophys. J. Int. 160, 849–854.
Gripp, A.E., Gordon, R.G., 1990. Current plate velocities relative to the hotspots incorporating the NUVEL-1 global plate motion model. Geophys. Res. Lett. 17, 1109–1112.
Gripp, A.E., Gordon, R.G., 2002. Young tracks of hotspots and current plate velocities. Geophys. J. Int. 150, 321–361.
Guzmán-Speziale, M., 1995. Hypocentral cross-sections and arc-trench curvature. Geofís. Int. 34, 131–141.
Guzmán-Speziale, M., Pennington, W.D., Matumoto, T., 1989. The triple junction of the North America, Cocos, and Caribbean plates: seismicity and tectonics. Tectonics 8, 981–997.
Guzmán-Speziale, M., Meneses-Rocha, J.J., 2000. The North America–Caribbean plate boundary west of the Motagua-Polochic fault system: a fault jog in southeastern Mexico. J. S. Am. Earth Sci. 13, 459–468.
Guzmán-Speziale, M., Gómez, J.M., 2002. Comment on "A new estimate for present-day Cocos–Caribbean plate motion: Implications for slip along the Central American volcanic arc" by Charles DeMets. Geophys. Res. Lett. 29 http://dx.doi.org/10.1029/2002GL015011.
Guzmán-Speziale, M., Valdés-González, C.M., Molina, E., Gómez, J.M., 2005. Seismic activity along the Central America volcanic arc: is it related to subduction of the Cocos plate? Tectonophysics 400, 241–254.
Guzmán-Speziale, M., Gómez-González, J.M., 2006. Seismic strain rate along the middle America trench reveals significant differences between Cocos–North America and Cocos–Caribbean convergence. Geophys. J. Int. 166, 179–185.
Hanus, V., Vanek, J., 1978. Subduction of the Cocos plate and deep active fracture zones of Mexico. Geofís. Int. 17, 14–53.
Harlow, D.H., White, R.A., 1985. Shallow earthquakes along the volcanic chain in Central America: evidence for oblique subduction (abstract). Earthq. Notes 55, 28.
Hayes, G.P., Wald, D.J., Johnson, R.L., 2012. Slab1.0: a three-dimensional model of global subduction zone geometries. J. Geophys. Res. 117, B01302. http://dx.doi.org/10.1029/2011JB008524.
Husker, A., Kostoglodov, V., Cruz-Atienza, V.M., Legrand, D., Shapiro, N., Payero, J.S., Campillo, M., Huesca-Pérez, E., 2012. Temporal variations of non-volcanic tremor (NVT) locations in the Mexican subduction zone: finding the NV sweet spot. Geochem. Geophys. Geosyst. 13, Q03011. http://dx.doi.org/10.1029/2011GC003916.
Iglesias, A., Singh, S.K., Lowry, A.R., Santoyo, M., Kostoglodov, V., Larson, K.M., Franco-Sánchez, S.I., 2004. The silent earthquake of 2002 in the Guerrero seismic gap, Mexico (Mw=7.6): Inversion of slip on the plate interface and some implications. Geofís. Int. 43, 309–317.
International Seismological Centre, 2012. On-line Bulletin. International Seismological Centre, Thatcham, United Kingdom. http://www.isc.ac.uk.
Jarrard, R.D., 1986. Relations among subduction parameters. Rev. Geophys. 24, 217–284.
Jording, A., Ferrari, L., Arzate, J., Jödicke, H., 2000. Crustal variations and terrane boundaries in southern Mexico as imaged by magnetotelluric transfer functions. Tectonophysics 327, 1–13.
Jost, M.L., Herrmann, R.B., 1989. A student's guide to and review of moment tensors. Seismol. Res. Lett. 60, 37–57.
Julian, B.R., Miller, A.D., Foulger, G.R., 1998. Non-double-couple earhquakes 1 theory. Rev. Geophys. 36, 525–549.
Kostoglodov, V., Ponce, L., 1994. Relationship between subduction and seismicty in the Mexican part of the Middle America trench. J. Geophys. Res. 99, 729–742.
Kostoglodov, V., Husker, A., Shapiro, N.M., Payero, J.S., Campillo, M., Cotte, N., Clayton, R., 2010. The 2006 slow slip event and nonvolcanic tremor in the Mexican subduction zone. Geophys. Res. Lett. 37, L24301. http://dx.doi.org/10.1029/2010GL045424.
LaFemina, P., Dixon, T.H., Govers, R., Norabuena, E., Turner, H., Saballos, A., Mattioli, G., Protti, M., Strauch, W., 2009. Fore-arc motion and Cocos Ridge collision in Central America. Geochem. Geophys. Geosyst. 10, Q05S14. http://dx.doi.org/10.1029/2008GC002181.
LeFevre, L.V., McNally, K.C., 1985. Stress distribution and subduction of aseismic ridges in the Middle America subduction zone. J. Geophys. Res. 90, 4495–4510.
Lemoine, A., Madariaga, R., Campos, J., 2002. Slab-pull and slab-push earthquakes in the Mexican, Chilean and Peruvian subduction zones. Phys. Earth Planet. Inter. 132, 157–175.
Lyon-Caen, H., Barrier, E., Laserre, C., Franco, A., Arzu, I., Chiquin, L., Chiquin, M., Duquesnoy, T., Flores, O., Galicia, O., Luna, J., Molina, E., Porras, O., Requena, J., Robles, V., Romero, J., Wolf, R., 2006. Kinematics of the North American–Caribbean–Cocos plates in Central America from new GPS measurements across the Polochic-Motagua fault system. Geophys. Res. Lett. 33, L19309. http://dx.doi.org/10.1029/2006GL027694.
Malfait, B.T., Dinkelman, M.G., 1972. Circum-Caribbean tectonic and igneous activity and the evolution of the Caribbean plate. Geol. Soc. Am. Bull. 83, 251–272.
McCaffrey, R., 1992. Oblique plate convergence, slip vectors, and forearc deformation. J. Geophys. Res. 97, 8905–8915.
McCaffrey, R., 1994. Global variability in subduction thrust zone-forearc systems. Pure Appl. Geophys. 142, 173–224.
Melgar, D., Pérez-Campos, X., 2011. Imaging the moho and subducted oceanic crust at the isthmus of Tehuantepec, Mexico, from receiver functions. Pure Appl. Geophys. 168, 1449–1460.
Mena, M., de la Fuente, M., Morán, D., Espíndola, J.M., Núñez-Cornú, F., Medina, F., 1995. Anomalías gravimétricas y espesor de la corteza en la región de Oaxaca. Geofís. Int. 34, 79–91.
Miller, A.D., Foulger, G.R., Julian, B.R., 1998. Non-double-couple earhquakes 2 observations. Rev. Geophys. 36, 551–568.
Minster, J.B., Jordan, T.H., 1978. Present-day plate motions. J. Geophys. Res. 83, 5331–5354.

Please cite this article in press as: Guzmán-Speziale, M., Zúñiga, F.R., Differences and similarities in the Cocos–North America and Cocos–Caribbean convergence, as revealed by seismic moment tensors, Journal of South American Earth Sciences (2015), http://dx.doi.org/10.1016/j.jsames.2015.10.002

Molina-Garza, R., Urrutia-Fucugauchi, J., 1993. Deep crustal structure of central Mexico derived from interpretation of Bouguer gravity anomaly data. J. Geodyn. 17, 181–201.

Molina-Garza, R.S., Geissman, J.W., Wayrzyniec, T.F., Peña Alonso, T.A., Iriondo, A., Weber, B., 2015. Geology of the coastal Chiapas (Mexico) Miocene plutons and the Tonalá shear zone: syntectonic emplacement and rapid exhumation during sinistral transpression. Lithosphere 7, 257–274. http://dx.doi.org/10.1130/L409.1.

Molnar, P., Sykes, L.R., 1969. Tectonics of the Caribbean and Middle America regions from focal mechanisms and seismicity. Geol. Soc. Am. Bull. 80, 1639–1684.

Muehlberger, W.R., Ritchie, A.W., 1975. Caribbean-Americas plate boundary in Guatemala and southern Mexico as seen on Skylab IV orbital photography. Geology 3, 232–235.

Pacheco, J.F., Sykes, L.R., Scholz, C.H., 1993. Nature of seismic coupling along simple plate boundaries of the subduction type. J. Geophys. Res. 98, 14133–14159.

Pardo, M., Suárez, G., 1995. Shape of the subducted Rivera and Cocos plates in southern Mexico: seismic and tectonic implications. J. Geophys. Res. 100, 12357–12373.

Payero, J.S., Kostoglodov, V., Shapiro, N., Mikumo, T., Iglesias, A., Pérez-Campos, X., Clayton, R.W., 2008. Nonvolcanic tremor observed in the Mexican subduction zone. Geophys. Res. Lett. 35, L07305. http://dx.doi.org/10.1029/2007GL032877.

Pérez-Campos, X., Kim, Y.H., Husker, A., Davis, P.M., Clayton, R.W., Iglesias, A., Pacheco, J.F., Singh, S.K., Manea, V.C., Gurnis, M., 2008. Horizontal subduction and truncation of the Cocos plate beneath central Mexico. Geophys. Res. Lett. 35, L18303. http://dx.doi.org/10.1029/2008GL035127.

Plafker, G., 1976. Tectonic aspects of the Guatemala earthquake of 4 February 1976. Science 193, 1201–1208.

Protti, M., Mcnally, K., 1994. The geometry of the Wadati-Benioff zone under southern Central America and its tectonic significance: results from a high-resolution local seismographic network. Phys. Earth Planet. Inter. 84, 271–287.

Rebollar, C., Espíndola, V.H., Uribe, A., Mendoza, A., Pérez-Vertti, A., 1999. Distributions of stresses and geometry of the Wadati-Benioff zone under Chiapas, Mexico. Geofís. Int. 38.

Rodriguez, M., DeMets, C., Rogers, R., Tenorio, C., Hernandez, D., 2009. A GPS and modelling study of deformation in northern Central America. Geophys. J. Int. 178, 1733–1754.

Siebert, L., Simkin, T., 2002. Volcanoes of the World: an Illustrated Catalog of Holocene Volcanoes and Their Eruptions. Smithsonian Institution, Global Volcanism Program Digital Information Series, GVP-3. Neotectonics of North America, Geological Society of America, Boulder, CO, pp. 323–338. http://www.volcano.si.edu/world/.

Singh, S.K., Mortera, F., 1991. Source time functions of large mexican subduction earthquakes, morphology of the Benioff zone, age of the plate, and their tectonic implications. J. Geophys. Res. 96, 21487–21502.

Smith, W.H.F., Wessel, P., 1990. Gridding with continuous curvature splines in tension. Geophysics 55, 293–305.

Suárez, G., Monfret, T., Wittinger, G., David, C., 1990. Geometry of subduction and depth of the seismogenic zone in the Guerrero gap, Mexico. Nature 345, 336–338.

Uyeda, S., 1982. Subduction zones: an introduction to comparative subductology. Tectonophysics 81, 133–159.

Uyeda, S., Kanamori, H., 1979. Back-arc opening and the mode of subduction. J. Geophys. Res. 84, 1049–1061.

Valdés-González, C.M., Meyer, R.P., 1996. Seismic structure between the Pacific coast and Mexico City from the Petatlán earthquake (M_s=7.6) aftershocks. Geofís. Int. 35, 377–401.

Wessel, P., Smith, W.H.F., 1991. Free software helps map and display data. EOS Trans. Am. Geophys. Union 72, 441.

Wessel, P., Smith, W.H.F., Scharroo, R., Luis, J.F., Wobbe, F., 2013. Generic mapping tools: improved version released. EOS Trans. Am. Geophys. Union 94, 409–410.

White, R., Harlow, D.H., 1993. Destructive upper-crustal earthquakes in Central America since 1900. Bull. Seismol. Soc. Am. 83, 1115–1142.

Please cite this article in press as: Guzmán-Speziale, M., Zúñiga, F.R., Differences and similarities in the Cocos–North America and Cocos–Caribbean convergence, as revealed by seismic moment tensors, Journal of South American Earth Sciences (2015), http://dx.doi.org/10.1016/j.jsames.2015.10.002